Inorganic Chemistry

Article

pubs.acs.org/IC

Structural Diversity in Coordination Self-Assembled Networks of a Multimodal Ligand Azacalix[4]pyrazine

Jin-Cheng Wu,[†] Liang Zhao,*[,‡] De-Xian Wang,[†] and Mei-Xiang Wang*[,†,‡]

[‡]The Key Laboratory of Bioorganic Phosphorus Chemistry & Chemical Biology (Ministry of Education), Department of Chemistry, Tsinghua University, Beijing 100084, China

[†]Beijing National Laboratory for Molecular Sciences, CAS Key Laboratory of Molecular Recognition and Function, Institute of Chemistry, Chinese Academy of Sciences, Beijing 100190, China

Supporting Information

ABSTRACT: We report herein the synthesis of a new heteracalixaromatic compound, tetramethylazacalix[4]pyrazine (**TAPz**), and its coordination self-assemblies with metal and metal cluster centers. Structural characterization of **TAPz** has shown that its conformation is fluxional in solution but exhibits a dominant 1,3-alternate configuration in the crystalline solid state, wherein its convergent chelating coordination sites are orthogonal to the 120°-angled bridging sites, thus forming a unique multimodal ligand. Compound **TAPz** reacting with silver, zinc metal centers, and Cu_xI_x cluster centers leads to the construction of diverse coordination network structures in **1**−**5** including honeycomb, Kagomé, α-quartz, and cavity-involved two-dimensional layers. The structural diversity of these network structures is conducted by different combination modes between the chelation bonding sites of **TAPz** and metal or metal cluster centers. This system may afford deeper insight on the fantastic use of macrocyclic compounds on the designed synthesis of coordination network structures through the proper arrangement of their coordination sites.

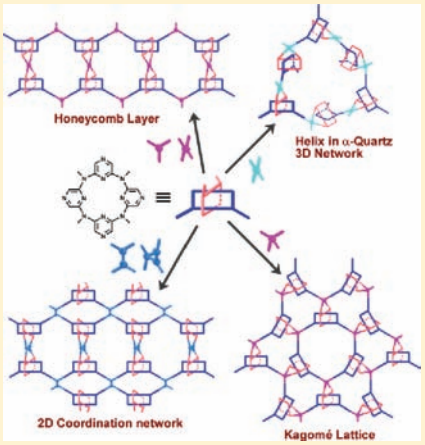

INTRODUCTION

The synthesis of coordination self-assembled supramolecular architectures[1] including two- and three-dimensional (3D) discrete ensembles and polymeric networks has long captivated chemists because of their wide variety of applications, including molecular recognition,[2] catalysis,[3] gas storage,[4] and stabilization of reactive materials and unstable species through cavity confinement.[5] In this regard, how to controllably and efficiently achieve structural diversity in metal−ligand self-assembled structures and thus tune their physical properties based on the structure−property relationship has become a significant task. One approach is to utilize multimodal bridging ligands that differ from more traditional tri- and tetradentate bridging systems in that they offer chemically distinct binding sites, both chelating and monodentate.[6] The multimodal ligand facilitates the control over network formation through the precise arrangement of metal centers by the hierarchical coordination ability of chelating and bridging sites. For example, 2,2′-bipyrazine can serve as a multimodal ligand to connect with silver(I) centers to generate a chiral coordination network with diamondoid topology,[7] in contrast to the common chelation behavior of the ligand 2,2′-bipyridine.

On the other hand, supramolecular networking of macrocyclic organic compounds has received considerable attention in recent years because of their high selectivity for specific metal ions and small molecules.[8] These features make such network structures attractive candidates for nanoscale chemical sensing applications. Meanwhile, the macrocyclic skeleton provides an excellent platform to sterically arrange different coordination sites in a special way, in contrast to often-used planar multidentate organic ligands. In the past decade, we have carried out systematic studies on the synthesis of heteracalixaromatics such as nitrogen- and oxygen-bridged calixpyridines,[9] calixpyrimidines,[10] and calixtriazines.[11] The structure studies of these macrocycles have explored unique structural characteristics distinct from conventional methylene-bridged calixarenes, mostly derived from alterable hybrid configurations (such as sp^2 and/or sp^3 for nitrogen) of heteroatoms and variable degrees of conjugation between heteroatoms and adjacent aromatics.[12] Because of the strong electron-donating nature of N(R) bridging moieties, azacalixheteroaromatics possess a good coordination ability to bond to metal ions. For example, tetramethylazacalix[4]-pyridine shows a good selectivity for recognition of the zinc ion.[13] We thus targeted the synthesis and coordination self-assembly study of tetramethylazacalix[4]pyrazine (**TAPz**), which features a macrocyclic skeleton and contains four pyrazinyl rings. In view of the dominant 1,3-alternate conformation in a lot of reported azacalix[4]aromatics,[9] **TAPz** may act as a novel multimodal ligand because its chelating sites are perpendicular to the bridging sites, as shown in Scheme 1. In this way, the coalescence between **TAPz** and different

Received: January 11, 2012
Published: March 2, 2012

   dx.doi.org/10.1021/ic3000679 | *Inorg. Chem.* 2012, 51, 3860−3867

Scheme 1. Possible Coordination Modes of Azacalix[4]pyrazine TAPz

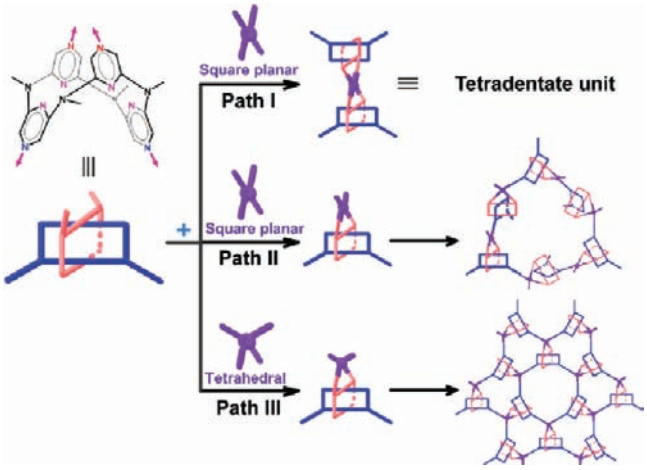

geometrical metal centers and the further self-assembly can be conceptually classified into three paths. In path I, two **TAPz** ligands bond to a square-planar metal center via its chelating sites, resulting in the formation of a tetradentate donor building block. The further self-assembly of this building block is dependent on the second metal center (acceptor). If the square-planar metal center is only chelated by one **TAPz** ligand (path II), the resulting building block owns two acceptor sites and two donor sites, which are orthogonal to each other. Consequently, a complementary combination of this building block can possibly engender the formation of a helical structure. However, when a tetrahedral metal center is employed, a Kagomé lattice is likely constructed as path III in Scheme 1. Herein, we report the synthesis and structural characterization of macrocyclic compound **TAPz** and its coordination self-assembly with different geometrical metal centers and clusters. Diverse coordination networks such as the honeycomb layer, Kagomé lattice, and α-quartz 3D chiral network are synthesized in complexes **1**−**5** as expected in Scheme 1.

EXPERIMENTAL SECTION

All chemicals were used as received commercially. The consumed solvents were processed according to standard procedures otherwise noticed. ^{1}H and ^{13}C NMR spectra were recorded at 300 MHz on a Bruker DMX-300 spectrometer. Electrospray ionization mass spectrometry (ESI-MS) spectra of complexes were measured on a Shimadzu LC-MS2010 mass spectrometer. IR spectra were measured on a Jasco FTIR-4800 spectrometer.

***N*^{2},*N*^{6}-Dimethylpyrazine-2,6-diamine (A).** 2,6-Dichloropyrazine (29.80 g, 0.20 mol) and a 25−30% aqueous solution of methylamine (220 mL) were added to a sealed tube. The reaction mixture was stirred at 180 °C (oil bath temperature) for 24 h and then allowed to cool to room temperature. The solvent CH_2Cl_2 (400 mL) was added, and the organic layer was separated, while the aqueous phase was further extracted by CH_2Cl_2 (200 mL × 3). The combined organic solution was dried over anhydrous Na_2SO_4. After removal of the solvent, the residue was chromatographed on a silica gel column (100−200) with a mixture of ethyl acetate and dichloromethane (1:4,v/v) as the eluent to give **A** as a green oil (20.25 g). Yield: 73%. Compound **A** is easily oxidized in air, so it should be stored in a refrigerator with the protection of argon gas. **A**: mp 69−70 °C; ^{1}H NMR (300 MHz, $CDCl_3$) δ 7.19 (s, 2H), 3.38 (s, 2H), 2.90 (s, 6H); ^{13}C NMR (75 MHz, $CDCl_3$) δ 154.1, 117.8, 28.5; IR (KBr) 3328, 3260, 3078, 1546 cm^{-1}; ESI-MS m/z 139.1 ([M + H]$^+$). Anal. Calcd for $C_6H_{10}N_4$: m/z 138.0905. Found: m/z 138.0907.

***N*^{2},*N*^{6}-Bis(6-chloropyrazin-2-yl)-*N*^{2},*N*^{6}-dimethylpyrazine-2,6-diamine (B).** In a round-bottomed flask charged with dry 1,4-dioxane (200 mL), sodium hydride (24.00 g, 1.0 mol) and **A** (6.90 g, 0.05 mol) were added successively. The reaction mixture was refluxed for 12 h and then allowed to cool to room temperature. 2,6-Dichloropyrazine (22.35 g, 0.15 mol) was added to the reaction mixture quickly, which was refluxed for 3 h. The flask was cooled to room temperature and subsequently placed in an ice−water bath. A saturated aqueous solution of ammonium chloride (50 mL) was added slowly to decompose excessive sodium hydride. Water (1000 mL) was added to the mixture and stirred for a further 1 h. The crude products were isolated upon filtration, which were then dissolved in dichloromethane and dried over anhydrous Na_2SO_4. After filtration and removal of the solvent, the crude product was purified by column chromatography (silica gel, 1:3 EtOAc/CH_2Cl_2), giving compound **B** as a pale-yellow solid. Yield: 88%. **B**: mp 164−165 °C; ^{1}H NMR (300 MHz, $CDCl_3$) δ 8.58 (s, 2H), 8.34 (s, 2H), 8.16 (s, 2H), 3.63 (s, 6H); ^{13}C NMR (75 MHz, $CDCl_3$) δ 151.9, 150.0, 146.4, 135.9, 134.2, 129.4, 35.4; IR (KBr) 1570, 1536, 1515, 1173, 1157 cm^{-1}; MS (MALDI-TOF) m/z 363 ([M + H]$^+$). Anal. Calcd for $C_{14}H_{12}Cl_2N_8$: C, 46.30; H, 3.33; N, 30.85. Found: C, 46.37; H, 3.33; N, 30.56.

***N*^{2}-(6-Chloropyrazin-2-yl)-*N*^{2},*N*^{6}-dimethyl-*N*^{6}-[6-[methyl[6-(methylamino)pyrazin-2-yl]amino]pyrazin-2-yl]pyrazine-2,6-diamine (C).** Compounds **A** (0.276 g, 2 mmol) and **B** (0.726 g, 2 mmol), $Pd_2(dba)_3$ (0.184 g, 0.2 mmol), 1,3-bis(diphenylphosphino)-propane (dppp; 0.082 g, 0.2 mmol), and ^{t}BuONa (0.576 g, 6 mmol) were added in a round-bottomed flask, and the system was flushed by argon gas three times. Dry toluene (400 mL) was filled in the flask via a syringe with stirring. The reaction mixture was heated to 70 °C and stirred for 4 h. After filtration, the solvent of filtrate was removed, and the resulting residue was chromatographed on silica gel (100−200) with a mixed solution of acetone and dichloromethane (1:3, v/v) as the eluent, producing **C** as a light-green solid (0.438 g) with recovery of a part of **B** (0.223 g, 31%). Yield: 47%. **C**: mp 180−181 °C; ^{1}H NMR (300 MHz, $CDCl_3$) δ 8.64 (s, 1H), 8.42 (s, 1H), 8.41 (s, 1H), 8.17 (s, 1H), 8.12 (s, 1H), 8.10 (s, 1H), 7.85 (s, 1H), 7.58 (s, 1H), 4.59 (br, 1H), 3.64 (s, 3H), 3.59 (s, 3H), 3.56 (s, 3H), 2.98 (d, J = 5.1 Hz, 3H); ^{13}C NMR (75 MHz, $CDCl_3$) δ 53.7, 152.2, 151.1, 150.9, 150.4, 150.0, 146.3, 135.1, 134.3, 130.1, 129.9, 127.4, 127.2, 124.5, 123.9, 35.4, 35.3, 35.2, 28.5; IR (KBr) 3436, 1563, 1529, 1512, 1479, 1405 cm^{-1}; MS (MALDI-TOF) m/z 465 ([M + H]$^+$). Anal. Calcd for $C_{20}H_{21}ClN_{12}$: C, 51.67; H, 4.55; N, 36.15. Found: C, 51.25; H, 4.54; N, 36.15.

Tetramethylazacalix[4]pyrazine (TAPz) and Octamethylazacalix[8]pyrazine. A round-bottomed flask was charged with compound **C** (0.927 g, 2 mmol), $Pd_2(dba)_3$ (0.184 g, 0.2 mmol), 2-dicyclohexylphosphino-2′-(*N*,*N*-dimethylamino)biphenyl (DavePhos; 0.236 g, 0.6 mmol), and Cs_2CO_3 (6.52 g, 20 mmol). The system was flushed via argon gas three times. Dry 1,4-dioxane (400 mL) was injected in the flask via a syringe with stirring. The reaction mixture was refluxed for 4 h and then cooled to room temperature. After filtration and removal of the solvent, the resulting residue was chromatographed on silica gel (100−200) with a mixed eluent solution of acetone and chloroform in a ratio of 2:3 to 6:1, giving **TAPz** as a pale-yellow solid (0.181 g) and an octamer compound (pale-yellow solid, 0.265 g). Yield: 21% (**TAPz**), 31% (octamer). Single crystals of **TAPz** were deposited by diffusing ethyl acetate into its chloroform solution. **TAPz**: mp 210−211 °C; ^{1}H NMR (300 MHz, $CDCl_3$) δ 7.88 (s, 8H), 3.31 (s, 12H); ^{13}C NMR (75 MHz, $CDCl_3$) δ 153.8, 131.1, 35.9; IR (KBr) 1572, 1535, 1475, 1431, 1413 cm^{-1}; MS (MALDI-TOF) m/z 429 ([M + H]$^+$), 451 ([M + Na]$^+$). Anal. Calcd for $C_{20}H_{20}N_{12}$: C, 56.07; H, 4.71; N, 39.23. Found: C, 55.97; H, 4.72; N, 39.38. **Octamer**: mp 224−225 °C; ^{1}H NMR (300 MHz, $CDCl_3$) δ 8.19 (s, 16H), 3.57 (s, 24H); ^{13}C NMR (75 MHz, $CDCl_3$) δ 150.6, 128.8, 35.0; IR (KBr) 1572, 1515, 1472, 1412 cm^{-1}; MS (MALDI-TOF) m/z 857.7 ([M + H]$^+$). Anal. Calcd for $C_{40}H_{40}N_{24}$: C, 56.07; H, 4.71; N, 39.23. Found: C, 56.47; H, 4.88; N, 39.07.

{[$Ag_{1.5}$(TAPz)](CF_3SO_3)$_{1.5}$·1.5CH_3CN·H_2O}$_n$ (1). Prismatic yellow-green crystals of **1** were obtained by diffusing ethyl acetate into the

dx.doi.org/10.1021/ic3000679 | Inorg. Chem. 2012, 51, 3860−3867

Table 1. Crystallographic Data of TAPz and Complexes 1−5

	TAPz	1	2	3	4[c]	5
formula	$C_{41}H_{44}N_{24}O$	$C_{24.5}H_{26.5}F_{4.5}N_{13.5}O_{5.5}S_{1.5}Ag_{1.5}$	$C_{20}H_{25}N_{13.5}O_7\ Ag_{1.5}$	$C_{80}H_{80}B_4\ F_{16}N_{48}O_{0.5}Ag_4$	$C_{22}H_{20}F_6N_{12}O_6\ S_2Zn$	$C_{20}H_{20}N_{12}Cu_{2.5}I_{2.5}$
fw	889.00	893.49	728.33	2500.64	791.99	904.58
cryst syst	triclinic	monoclinic	monoclinic	monoclinic	trigonal	orthorhombic
space group	$P\bar{1}$	$C2/c$	$C2/c$	$P2_1/n$	$P3_121$	$Pmmn$
a [Å]	10.115(2)	27.535(6)	28.615(6)	18.797(4)	15.729(2)	24.142(2)
b [Å]	10.646(2)	14.067(3)	13.315(3)	18.883(4)	15.729(2)	35.780(7)
c [Å]	20.672(4)	18.359(4)	18.187(4)	31.934(6)	12.403(3)	9.209(1)
α [deg]	75.51(3)	90	90	90	90	90
β [deg]	88.28(3)	112.81(3)	113.32(3)	90.69(3)	90	90
γ [deg]	76.32(3)	90	90	90	120	90
V [Å^3]	2093.0(7)	6555(2)	6364(2)	11334(4)	2657.6(8)	7955(2)
ρ [g/cm^3]	1.411	1.811	1.518	1.465	1.485	1.511
μ [cm^{-1}]	0.096	1.088	0.990	0.770	0.895	3.294
Z	2	8	8	4	3	8
R1[a] [$I > 2\sigma(I)$]	0.0646	0.0790	0.0666	0.1330	0.0528	0.0729
wR2[b] (all data)	0.1885	0.1791	0.1653	0.3324	0.1251	0.2069
GOF	1.083	1.163	1.079	1.142	1.169	1.040

[a] $R1 = \sum||F_o| - |F_c||/\sum|F_o|$. [b] $wR2 = \{\sum[w(F_o^2 - F_c^2)^2]/\sum[w(F_o^2)^2]\}^{1/2}$. [c] Flack parameter = 0.070(17).

Scheme 2. Synthesis of Compound TAPz

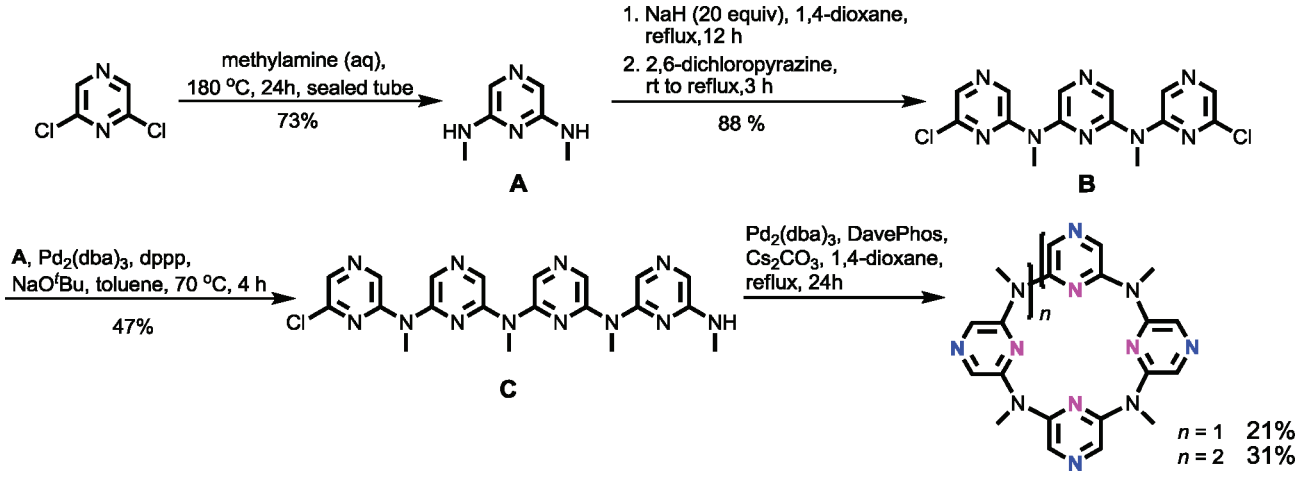

mixed solution of **TAPz** (8.5 mg, 0.02 mmol) in chloroform (1 mL) and silver triflate (5.2 mg, 0.02 mmol) in acetonitrile (1 mL).

{$Ag_{1.5}$(TAPz)]$(NO_3)_{1.5}$·2.5H_2O}$_n$ (2). Prismatic yellow-green crystals of **2** were obtained according to the same synthetic method as that for the preparation of **1** by use of silver nitrate reacting with compound **TAPz**.

{[Ag_4(TAPz)$_4$]$(BF_4)_4$·solvent}$_n$ (3). Diffusion of ethyl acetate into the mixed solution of **TAPz** (8.5 mg, 0.02 mmol) in chloroform (1 mL) and silver tetrafluoroborate (4.0 mg, 0.02 mmol) in acetonitrile (1 mL) yielded yellow-green crystals of **3**.

{[Zn(TAPz)]$(CF_3SO_3)_2$·solvent}$_n$ (4). After the chloroform/methanol (1:1) solution of **TAPz** (8.5 mg, 0.02 mmol) was mixed with zinc triflate (7.3 mg, 0.02 mmol) in methanol, acetonitrile and ethyl acetate were sequentially diffused in the reaction mixture. After several days, pale-yellow hexagonal prismatic crystals of **4** were obtained.

{[$(Cu_3I_3)_{0.5}(Cu_2I_2)_{0.5}$(TAPz)]·solvent}$_n$ (5). Compound **TAPz** (8.5 mg, 0.02 mmol) was dissolved in a mixed solvent of chloroform (1 mL) and acetonitrile (1 mL). CuI solids (9.1 mg, 0.05 mmol) were added to the above mixed solution to obtain a mixture. Slow diffusion of benzene into the mixture generated blocklike green crystals of **5**.

X-ray Crystallography. Data for **TAPz** and coordination complexes **1**−**5** were collected at 173 K with Mo Kα radiation (λ = 0.71073 Å) on a Rigaku Saturn 724+ CCD diffractometer with frames of oscillation range 0.5°. All structures were solved by direct methods, and non-hydrogen atoms were located from difference Fourier maps. All non-hydrogen atoms were subjected to anisotropic refinement by full-matrix least squares on F^2 by using the *SHELXTL* program otherwise noted in the Supporting Information. Corrections of the X-ray data for **3**−**5** were processed by the *SQUEEZE* program[14] because of the disordered solvent molecules. The *X-Seed* program[15] was used to generate the X-ray structural diagrams pictured in this paper. The parameters for the crystal data and X-ray structure analysis are summarized in Table 1.

RESULTS AND DISCUSSION

Synthesis and Structural Characterization of TAPz. Our previous systematic studies on the synthesis of azacalix[n]pyridines (n = 4−10) have indicated that the fragment coupling approach is a highly efficient synthetic method to construct macrocyclic azacalixaromatics.[16] However, the synthesis of compound **TAPz** was unsuccessful by the [3 + 1] synthetic procedure. The reaction between the linear trimer compound **B** and the diaminated compound **A** merely produced the linear tetramer compound **C** and its dehalogenated analogue rather than the desired macrocyclic compound **TAPz** (Scheme 2). We subsequently envisioned that the linear tetramer compound **C**, which incorporates four pyrazine rings and contains a Cl terminal and a NH(Me) terminal, may

dx.doi.org/10.1021/ic3000679 | Inorg. Chem. 2012, 51, 3860−3867

undergo intramolecular macrocyclization to generate the target compound **TAPz**. A yield of 47% for **C** with a recovery of 31% trimer reactant **B** was accomplished by operating the palladium-catalyzed coupling reaction of **A** and **B** at 70 °C in toluene in the presence of dppp as the ligand and $NaOBu^t$ as the base. The reaction conditions of palladium-catalyzed macrocyclization of compound **C** were then optimized to obtain **TAPz** (see the Supporting Information). Moderate yields of **TAPz** (21%) and the octamer (31%) were finally achieved when the reaction was carried out in 1,4-dioxane in the presence of DavePhos and Cs_2CO_3. As far as we know, compound **TAPz** is the first example of all-pyrazine calixaromatic compounds.

The structure of **TAPz** was determined by NMR, elemental analysis, and X-ray crystallography. The ^1H and ^{13}C NMR spectra of **TAPz** exhibited only one set of signals, suggestive of a fluxional and promptly interconverted conformation for **TAPz** in solution. This conformational fluxionality may be ascribed to the small steric hindrance of the methyl groups on the $N-CH_3$ bridging moieties and the absence of strong conformation-stabilized intramolecular interactions. X-ray crystallographic studies revealed that **TAPz** featuring a macrocyclic scaffold adopts an 1,3-alternate conformation with two opposite aromatic rings at procumbent positions and the other two at perpendicular positions relative to the plane determined by four $N-CH_3$ moieties (Figure 1 and Table 2). It is noticeable

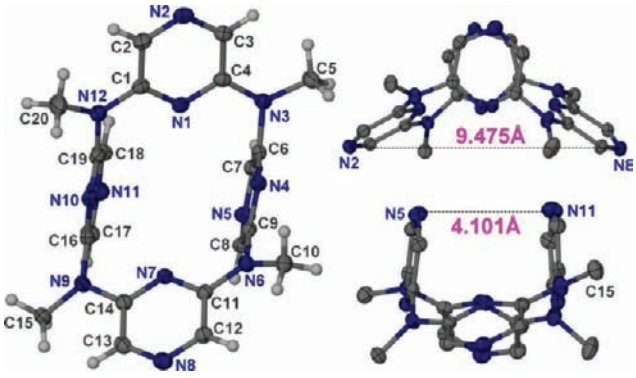

Figure 1. X-ray crystal structure of **TAPz** with a top view and two side views, respectively (50% probability thermal ellipsoids). There are two similar asymmetric macrocycles in the crystal structure of **TAPz**. Only one is shown here. Color scheme for atoms: C, black; H, gray; N, blue.

Table 2. Selected Bond Lengths, Distances, and Torsion Angles in the Crystal Structure of TAPz

$N-C_{Pz}$ or $N-C_{Py}$ (Å)		torsion angle (deg)	
N3–C4	1.376(3)	∠C5–N3–C4–C3	4.3
N3–C6	1.427(3)	∠C5–N3–C6–N4	87.5
N6–C9	1.412(3)	∠C10–N6–C9–N4	45.6
N6–C11	1.387(3)	∠C10–N6–C11–C12	26.4
N9–C14	1.378(3)	∠C15–N9–C14–C13	27.6
N9–C16	1.420(3)	∠C15–N9–C16–N10	126.7
N12–C19	1.419(3)	∠C20–N12–C19–N10	50.3
N12–C1	1.377(3)	∠C20–N12–C1–C2	20.2

that each bridging nitrogen atom exhibits a sp^2 electron configuration that is supported by the 360° bond angle summation for each bridging nitrogen atom.

Crystal Structures of Coordination Self-Assembled Complexes of TAPz. With the compound **TAPz** in hand, we next carried out coordination self-assembly studies of this macrocyclic ligand. Silver ion was utilized as a probe for the coordination self-assembly study of **TAPz** because of its versatile coordination geometries such as linear, trigonal, and tetrahedral. Coordination self-assembly of **TAPz** with $[CuI]_n$ metal clusters was also investigated because of various configurations of copper halides, such as rhomboid Cu_2X_2 dimers, cubane- or chairlike $[Cu_4X_4]$ tetramers, zigzag $[CuX]_n$ or $[Cu_3X_4]_n^{n-}$ chains, and ladder or ribbon $[Cu_2I_2]_n$ chains.[17] Zinc ion was employed for providing a special case of the octahedral coordination geometry in coordination self-assembly studies.

In the crystal structure of complex $\{[Ag_{1.5}(\mathbf{TAPz})](CF_3SO_3)_{1.5}\cdot 1.5CH_3CN\cdot H_2O\}_n$ (**1**), two independent silver centers are involved, and each one exhibits a different coordination geometry (Figure 2a). Ag1 is bonded in an octahedral

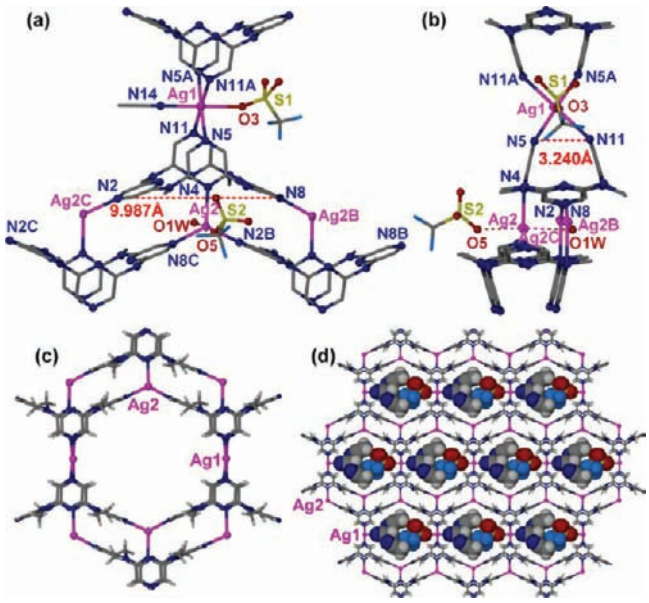

Figure 2. (a) Coordination environments of **TAPz** and silver atoms in complex **1** with atom labeling. Symmetry code: A, $1-x, y, {}^1/_2-z$; B, ${}^1/_2-x, y-{}^1/_2, {}^1/_2-z$; C, ${}^1/_2-x, y+{}^1/_2, {}^1/_2-z$. (b) Side view. (c) Hexagonal macrocycle constructed by silver atoms and **TAPz** ligands. (d) Double-walled honeycomb layer structure in **1**. Three acetonitrile molecules and one triflate shown in the space-filling model are embedded in each cell. Color scheme for atoms: Ag, purple; C, black; H, gray; O, red; N, blue; F, cyan.

configuration by two pairs of chelating nitrogen atoms of **TAPz** [Ag–N = 2.344(5)–2.678(8) Å], a triflate anion [Ag1–O3 = 2.541(8) Å], and an acetonitrile molecule [Ag1–N14 = 2.486(10) Å]. The coalescence between Ag1 and **TAPz** follows path I shown in Scheme 1, finally leading to the formation of a tetradentate coordinative unit. The silver atom Ag2 joins with such coordination donor units by the coordination of two outer pyrazinyl nitrogen atoms of **TAPz** [Ag2–N2 = 2.273(5) Å and Ag2–N8 = 2.286(5) Å] to produce a coordination hexagon (Figure 2c). Extension of the hexagons by the coordination of four divergent bonding sites of the tetradentate unit generates an infinite one-dimensional (1D) chain along the *b* direction with a series of hexagons arranged shoulder-by-shoulder. Such 1D coordination chain is cross-linked by the coordination between Ag2 and an inner pyrazinyl nitrogen atom N4 [2.374(5) Å] to result in a coordination honeycomb layer structure parallel to the *ab* plane (Figure 2d). Because of the contacts between Ag2 and the oxygen atom O5 of a triflate anion and the water

dx.doi.org/10.1021/ic3000679 | Inorg. Chem. 2012, 51, 3860–3867

molecule O1W, the coordination geometry of Ag2 could be properly expressed as a trigonal-bipyramidal conformation. In addition, three acetonitriles and a triflate anion are found to be accommodated in the void space of the hexagonal honeycomb cell, suggestive of the existence of porosity in this coordination network. Coordination self-assembly between silver nitrate and **TAPz** yielded complex $\{[Ag_{1.5}(\mathbf{TAPz})](NO_3)_{1.5}\cdot 2.5H_2O\}_n$ (**2**), which is isostructural with **1** but using nitrates and water molecules in place of triflates and acetonitrile molecules. It is well-known that the honeycomb layer structures have significant applications in gas adsorption[18] and have exhibited interesting photophysical[19] and magnetic properties in previously reported complexes.[20] The synthesis of complexes **1** and **2** spotlights a common strategy to construct the honeycomb network by use of a conformation rigid polydentate ligand.

In the above two silver complexes **1** and **2** of **TAPz**, the counteranions (triflate and nitrate) coordinate to silver metal centers and thus influence the self-assembly process between **TAPz** and silver atoms. We subsequently utilized silver tetrafluoroborate to carry out the coordination self-assembly study of **TAPz** in view of the weak coordination ability of BF_4^-. The reaction of **TAPz** with silver tetrafluoroborate in an 1:1 molar ratio in a mixed solvent of chloroform and acetonitrile yielded yellow crystals of $\{[Ag_4(\mathbf{TAPz})_4](BF_4)_4\cdot \text{solvents}\}_n$ (**3**), which comprises four independent tetrahedrally coordinated silver atoms (Ag1−Ag4), four **TAPz** ligands (**I**−**IV**), and four separate tetrafluoroborate anions. As shown in Figure 3a, three

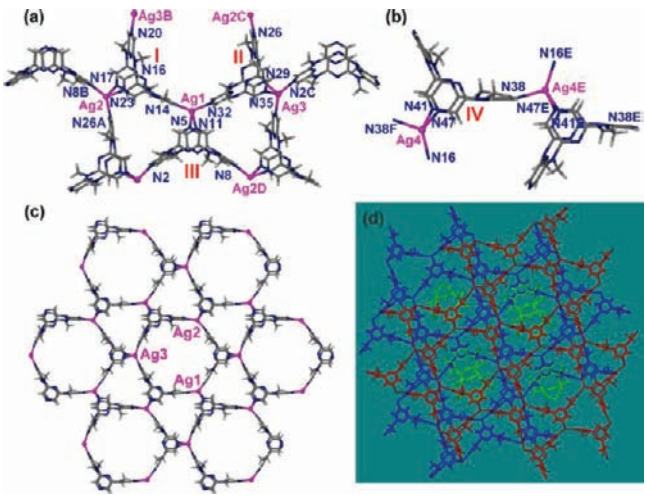

Figure 3. Crystal structure of **3**. (a) Coordination modes of three independent **TAPz** ligands (**I**−**III**) and coordination environments of Ag1, Ag2, and Ag3. (b) Infinite coordination chain composed of the ligand **IV** and silver atom Ag4. (c) 2D Kagomé network in **3** parallel to the *ac* plane. (d) 3D coordination network assembled by the ABAB Kagomé layers (blue and red) through the threading of a series of infinite coordination chains (green) along the *b* direction. Other ligands are omitted for clarity. Symmetry code: A, $x - {}^1/_2$, ${}^{11}/_2 - y$, $z - {}^1/_2$; B, $x - 1$, y, z; C, $x + {}^1/_2$, ${}^{11}/_2 - y$, $z + {}^1/_2$; D, $x + 1$, y, z; E, ${}^1/_2 - x$, $y - {}^1/_2$, $-z - {}^1/_2$; F, ${}^1/_2 - x$, $y + {}^1/_2$, $-z - {}^1/_2$. Color scheme for atoms: Ag, purple; C, black; H, gray; N, blue.

TAPz ligands (**I**−**III**) each chelate with a silver atom (Ag1−Ag3) via the outer nitrogen atoms of two opposite perpendicular pyrazine rings (N5−N11, N17−N23, and N29−N35) with Ag−N bond distances in the range of 2.367(10)−2.572(11) Å. Furthermore, the other two outer nitrogen atoms on the procumbent pyrazine rings of ligands **I**−**III** bond to two silver atoms with a contacting angle of approximately 120° [Ag−N = 2.213(10)−2.287(10) Å]. The assembly of such dendritic metal−organic building blocks results in a Kagomé lattice coordination layer parallel to the *ac* plane that contains interlaced three- and six-membered rings, as shown in Figure 3c. This synthesis follows path III in Scheme 1. The quasi-equilateral triangle in **3** is composed of three silver atoms (Ag1, Ag2, and Ag3) and three halves of **TAPz** ligands (**I**−**III**) with the Ag···Ag separation distances in the range of 9.82−9.96 Å. The connection of the three silver atoms Ag1−Ag3 by **I**−**III** via 120°-angled procumbent pyrazinyl nitrogen atoms leads to a distorted hexagon. Such Kagomé layers are stacked in an ABAB fashion with the interlayer separation of 9.44 Å along the *b* direction. As shown in Figure 3b, these parallel Kagomé layers are further consolidated by the threading of an infinite coordination chain that is composed of **IV** and Ag4 (Figure 3b), producing a pillared Kagomé 3D coordination network through the connection of Ag4 (thread)−N16 (layer). The Kagomé lattice has recently attracted much attention of theorists and chemists because of their geometry-related novel physical properties.[21] However, only a scant few examples of Kagomé topological metal−organic compounds were reported in the literature,[22] which behave as a kind of promising novel materials with interesting magnetic properties such as spin frustration, long-range antiferromagnetic ordering, and spin canting. The coordination between the well-designed ligand **TAPz** and a tetrahedral metal center as in complex **3** affords a new synthetic protocol for Kagomé lattices.

The self-assembly between **TAPz** and octahedral coordination metal ions was exemplified by the use of a zinc center, a common octahedral node in coordination self-assembly. Evaporation of the $CHCl_3/CH_3CN$/EtOAc mixed solution of **TAPz** and zinc triflate in a 1:1 ratio yielded colorless single crystals of $\{[Zn(\mathbf{TAPz})](CF_3SO_3)_2\cdot \text{solvents}\}_n$ (**4**). X-ray crystallographic analysis revealed that complex **4** crystallizes in a chiral trigonal space group of $P3_121$ (No. 152) with the Flack parameter equal to 0.070(17). The zinc center (Zn1) is surrounded by two C_2-related triflate anions at Zn1−O1 = 2.162(3) Å and three **TAPz** ligands—two in bridging fashion at Zn1−N6B = 2.116(3) Å and one in chelation mode at Zn1−N4 = 2.254(3) Å, being identical with the path II bonding scenario in Scheme 1. Although the four coordination nitrogen atoms are almost coplanar with Zn1 (Figure 4a), the remaining coordination vectors of the two bridging **TAPz** ligands form an angle of 67° (indicated as red arrows in Figure 4). Further linkage of the [Zn(*μ*-*N*,*N*′-**TAPz**)] chelation unit by the two 67°-angled divergent coordination nitrogen atoms generates a 3D coordination network with an *α*-quartz structure (Figure 4c). This network structure contains two kinds of trigonal channels derived from two types of helices (Figure 4c). The small trigonal channel, which is fully filled by triflate anions, is built up by a P-type (right-handed) single-stranded helix along a 3-fold screw axis through the linkage of zinc centers by a *μ*-N6 plus N4,N4A-chelating mode of **TAPz**. The big trigonal channel arises from two M-type (left-handed) chiral helixes. Each turn of the helix pitch is 24.806 Å, twice the length of the *c* axis. The quartz structure is a most stable form of silica, which has exhibited attractive physical properties because of its chirality and noncentrosymmetry, such as second-harmonic generation and piezoelectricity.[23]

Green block crystals of $\{[(Cu_3I_3)_{0.5}(Cu_2I_2)_{0.5}(\mathbf{TAPz})]\cdot \text{solvents}\}_n$ (**5**) were deposited through the diffusion of benzene into the mixed chloroform/acetonitrile solution of **TAPz**

dx.doi.org/10.1021/ic3000679 | *Inorg. Chem.* 2012, 51, 3860−3867

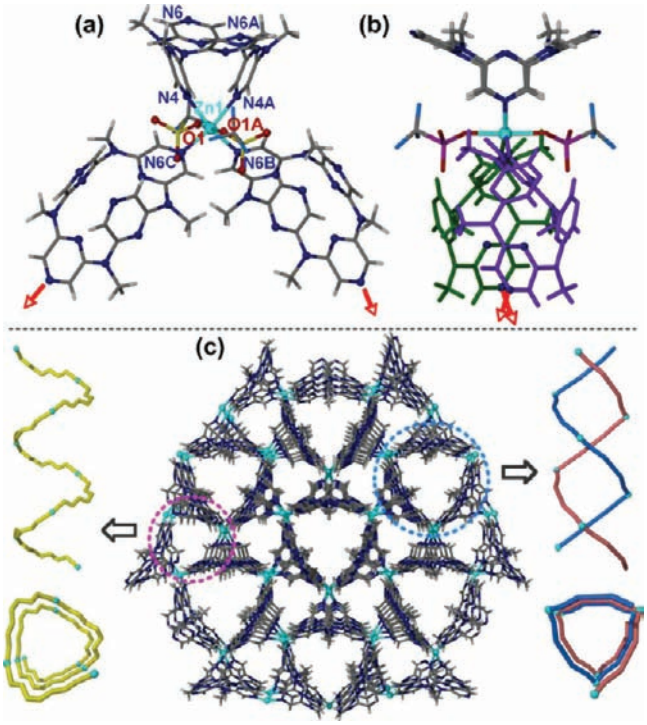

Figure 4. Crystal structure of **4**. (a) Coordination environment of the zinc center. Other ligands are omitted for clarity. Symmetry code: A, *y*, *x*, 2 − *z*; B, 1 − *y*, *x* − *y*, $^{1}/_{3}$ + *z*; C, *x* − *y*, 1 − *y*, $1^{2}/_{3}$ − *z*. (b) 90° Rotation view for illustrating two coordination vectors (red arrow) of the two bridged azacalix[4]pyrazine ligands. (c) 3D α-quartz structure in **4** containing a P-type helix of the trigonal channel (left) and a M-type double helix of the trigonal channel (right). Color scheme for atoms: Zn, light blue; C, black; H, gray; O, red; N, blue; F, cyan.

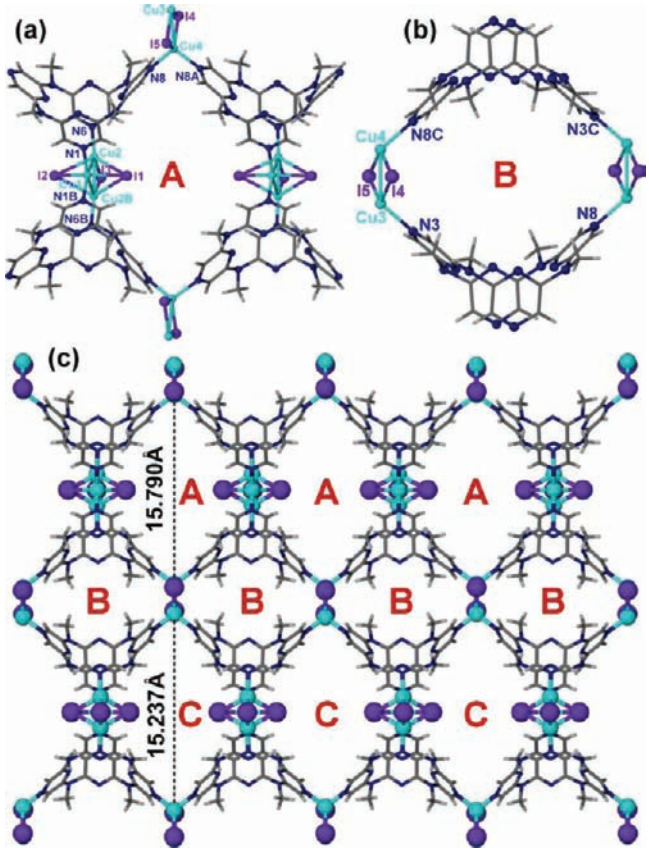

Figure 5. Crystal structure of **5**. (a) Cage **A** constructed by the linkage of **TAPz** via Cu_3I_3 and Cu_2I_2 clusters. (b) Cage **B** built from two **TAPz** ligands and two Cu_2I_2 clusters. (c) 2D coordination layer in **5** parallel to the *ab* plane. Other ligands are omitted for clarity. Symmetry code: A, $x - {}^{1}/_{2}$, 2 − *y*, 1 − *z*; B, *x*, $^{11}/_{2} - y$, *z*; C, 1 − *x*, 2 − *y*, 1 − *z*. Color scheme for atoms: Cu, light blue; I, violet; C, black; H, gray; N, blue.

and CuI. The single-crystal structure determination of **5** has explored two different copper iodide clusters, $[Cu_2I_2]$ and $[Cu_3I_3]$ (Figure 5). The $[Cu_2I_2]$ cluster is in a rhomboid dimer configuration with a mean Cu−I distance of 2.63 Å and a Cu3···Cu4 contact of 2.589(4) Å, which is much shorter than the sum of the van der Waals radii of the copper(I) ion (2.80 Å). This kind of $[Cu_2I_2]$ cluster is extensively shown in numerous reported copper halide complexes.[17] Remarkably, the Cu2···Cu2B separation in the $[Cu_3I_3]$ cluster is 2.441(4) Å, among the shortest distances of cuprophilic interaction observed to date in reported metal−organic hybrid complexes.[24] This short Cu−Cu separation may be attributed to the bridging effect of three iodides and an increased metallophilic attraction arising from iodide-donating electrons to the cuprous s orbitals that provide the bonding component of the cuprophilic interactions. As shown in Figure 5a, the Cu_3I_3 cluster is joined by two pairs of perpendicular pyrazinyl nitrogen atoms of the **TAPz** ligand at Cu−N = 2.000−2.049 Å, resulting in a dendritic unit. These dendritic units are further bridged by the Cu4 atom of the $[Cu_2I_2]$ rhomboid dimer at Cu4−N8 = 2.083 Å to generate a coordination cage **A** (Figure 5a). A similar bonding fashion but using the Cu3 atom at Cu3−N3 = 2.076 Å produces an almost identical coordination cage **C** (Figure 5c). In addition, **TAPz** ligands can be bridged by the $[Cu_2I_2]$ cluster through the coordination of two outer pyrazinyl nitrogen atoms with copper centers, engendering the formation of cage **B** (Figure 5b). These cages are arranged shoulder-by-shoulder and connected mutually to afford a two-dimensional (2D) coordination network parallel to the *ab* plane (Figure 5c).

Coordination Behaviors of TAPz. The above-reported coordination network structures of **TAPz** confirm the dominance of the 1,3-alternate conformation in the coordination self-assembly process of this macrocyclic ligand. When this macrocyclic ligand is used in coordination self-assembly, its coordination sites can be differentiated into two types: a pair of divergent extending sites and a pair of convergent chelating sites. As analyzed in Table 3, the two perpendicular pyrazine rings of the 1,3-alternate **TAPz** form an acute angle ($\angle V_1$−V_2) to chelate with a silver center (in **1**−**3**), a zinc center (in **4**), and a Cu_3I_3 cluster (in **5**). In contrast, the two procumbent rings constitute an obtuse angle ($\angle V_3$−V_4) to connect with metal centers and construct a coordination network with higher dimensionality, such as a honeycomb structure in **1** and **2**, a Kagomé lattice in **3**, a α-quartz structure in **4**, and an 2D metal cluster-centered coordination network in **4**. In the network structures of complexes **1**, **2**, and **5**, a square-planar metal or metal cluster center is doubly coordinated by the chelation sites of **TAPz**. This generates a new tetradentate donor building block, as shown in Scheme 1 (path I), which is further linked by another trigonal silver center in complexes **1** and **2** or a square-planar Cu_2I_2 center in **5** to construct a 2D coordination layer network in these three complexes. These kinds of network structures can be appropriately described as a donor + acceptor + donor building unit linked by metal or metal cluster centers. As to the paths II and III of **TAPz** in Scheme 1, the metal center is chelated by the **TAPz** ligand to form a acceptor + donor

dx.doi.org/10.1021/ic3000679 | *Inorg. Chem.* 2012, 51, 3860−3867

Table 3. Geometrical Parameters of TAPz in Its Free State and Coordination Complexes[a]

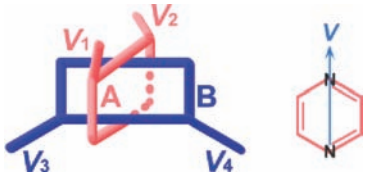

complex	$\angle V_1-V_2$ (deg)	$\angle V_3-V_4$ (deg)	$\angle A-B$ (deg)
TAPz	25.7	117.7	87.6
	27.4	116.9	88.2
1	29.7	135.9	89.6
2	31.5	118.8	88.3
3	32.4	114.3	89.1
	33.8	114.1	87.2
	31.8	115.4	90.3
	36.4	114.3	89.1
4	43.9	135.7	88.8
5	28.9	94.5	90.2

[a] $\angle V_m-V_n$ indicates the angle between two coordination vectors (V) of two opposite pyrazine rings. $\angle A-B$ represents the dihedral angle between two planes (pink and blue) that are determined by corresponding coordination vectors.

building unit. If the metal center is tetrahedral, its two pairs of acceptor sites are also orthogonal (such as in complex **3**). Therefore, the acquired conjoined acceptor + donor building unit owns two donor sites and two acceptor sites that are located on the same plane. A 2D Kagomé coordination network is thus achieved. However, when a square-planar metal center is applied, the two donor coordination sites of the conjoined acceptor + donor building unit are orthogonal to the acceptor sites, which account for the formation of a helix structure in complex **4**. In summary, the structural diversity in the above coordination networks of **TAPz** can be properly ascribed to the orthogonal arrangement of the coordination vectors V_1-V_2 (convergent) and V_3-V_4 (divergent) and different association modes between **TAPz** and metal centers.

CONCLUSION

In summary, a new pyrazine-all nitrogen-bridged calixaromatic, **TAPz**, was successfully synthesized by the fragment coupling method and structurally characterized. The 1,3-alternate conformation of the **TAPz** ligand affords both divergent and convergent coordination site pairs that are orthogonal to each other. The coordination self-assembly of **TAPz** with metal or metal cluster centers can produce both donor + acceptor and donor + acceptor + donor conjoined building units through three paths (I–III), which account for the formation of diverse coordination networks including the Kagomé lattice, α-quartz structure, and 2D capsule-involved layer in **1**–**5**. This study has illustrated the advantage of heteracalixaromatic skeletons to designedly construct unconventional multidentate coordinative ligands. These unique ligands feature a preorganized curved conformation and have good coodination ability and rigidity, thus facilitating their application in the design and synthesis of desired cavity-involved coordination networks. Our further goal is to construct new coordinative organic ligands based on the heteracalixaromatic skeleton and apply them in the construction of functional coordination networks.

ASSOCIATED CONTENT

Supporting Information

Experimental procedures and crystal structure determination details, IR and ^{1}H and ^{13}C NMR spectra, and X-ray crystallographic data for **TAPz** and **1**–**5** in CIF format. This material is available free of charge via the Internet at http://pubs.acs.org.

AUTHOR INFORMATION

Corresponding Author

*E-mail: zhaolchem@mail.tsinghua.edu.cn (L.Z.), wangmx@mail.tsinghua.edu.cn (M.-X.W.).

Notes

The authors declare no competing financial interest.

ACKNOWLEDGMENTS

We gratefully acknowledge financial support from the National Natural Science Foundation of China (Grants 21002057, 21132005, 21121004, and 91127006) and the National Basic Research Program of China (973 program, Grant 2011CB932501). This work is also supported by the Tsinghua University Initiative Scientific Research Program.

REFERENCES

(1) For reviews, see: (a) Leininger, S.; Olenyuk, B.; Stang, P. J. *Chem. Rev.* **2000**, *100*, 853. (b) Seidel, S. R.; Stang, P. J. *Acc. Chem. Res.* **2002**, *35*, 972. (c) Swiegers, G. F.; Malefetse, T. J. *Coord. Chem. Rev.* **2002**, *225*, 91. (d) Holliday, B. J.; Mirkin, C. A. *Angew. Chem., Int. Ed.* **2001**, *40*, 2022. (e) Cotton, F. A.; Lin, C.; Murillo, C. A. *Acc. Chem. Res.* **2001**, *34*, 759. (f) Fujita, M. *Chem. Soc. Rev.* **1998**, *27*, 417. (g) Lee, S. J.; Lin, W. *Acc. Chem. Res.* **2008**, *41*, 521. (h) Schwab, P. F. H.; Levin, M. D.; Michl, J. *Chem. Rev.* **1999**, *99*, 1863. (i) Fujita, M.; Tominaga, M.; Hori, A.; Therrien, B. *Acc. Chem. Res.* **2005**, *38*, 369. (j) Ward, M. D. *Chem. Commun.* **2009**, 4487. (k) Chakrabarty, R.; Mukherjee, P. S.; Stang, P. J. *Chem. Rev.* **2011**, *111*, 6810.

(2) (a) Kesanli, B.; Lin, W. *Coord. Chem. Rev.* **2003**, *246*, 305. (b) Yoshizawa, M.; Tamura, M.; Fujita, M. *J. Am. Chem. Soc.* **2004**, *126*, 6846. (c) Rebek, J. Jr. *Acc. Chem. Res.* **2009**, *42*, 1660. (d) Britt, D.; Furukawa, H.; Wang, B.; Glover, T. G.; Yaghi, O. M. *Proc. Natl. Acad. Sci. U.S.A.* **2009**, *106*, 20637.

(3) (a) Sanders, J. K. M. *Chem.—Eur. J.* **1998**, *4*, 1378. (b) Yoshizawa, M.; Kusukawa, T.; Fujita, M.; Yamaguchi, K. *J. Am. Chem. Soc.* **2000**, *122*, 6311. (c) Yoshizawa, M.; Tamura, M.; Fujita, M. *Science* **2006**, *312*, 251. (d) Merlau, M. L.; Del Pilar Mejia, M.; Nguyen, S. T.; Hupp, J. T. *Angew. Chem., Int. Ed.* **2001**, *40*, 4239. (e) Fiedler, D.; Leung, D. H.; Bergman, R. G.; Raymond, K. N. *Acc. Chem. Res.* **2005**, *38*, 349. (f) Pluth, M. D.; Bergman, R. G.; Raymond, K. N. *Science* **2007**, *316*, 85. (g) Gianneschi, N. C.; Nguyen, S. T.; Mirkin, C. A. *J. Am. Chem. Soc.* **2005**, *127*, 1644. (h) Lee, S. J.; Lin, W. *Acc. Chem. Res.* **2008**, *41*, 521. (i) Yoon, H. J.; Kuwabara, J.; Kim, J.-H.; Mirkin, C. A. *Science* **2010**, *330*, 66.

(4) (a) Batten, S. R.; Robson, R. *Angew. Chem., Int. Ed.* **1998**, *37*, 1460. (b) Eddaoudi, M.; Moler, D. B.; Li, H.; Chen, B.; Reineke, T. M.; O'Keeffe, M. O.; Yaghi, O. M. *Acc. Chem. Res.* **2001**, *34*, 319. (c) Moulton, B.; Zaworotko, M. J. *Chem. Rev.* **2001**, *101*, 1629. (d) Kitagawa, S.; Kitaura, R.; Noro, S. *Angew. Chem., Int. Ed.* **2004**, *43*, 2334. (e) Férey, G. *Chem. Soc. Rev.* **2008**, *37*, 191. (f) Wang, B.; Côté, A. P.; Furukawa, H.; O'Keeffe, M.; Yaghi, O. M. *Nature* **2008**, *453*, 207. (g) Fujita, M.; Kwon, Y. J.; Washizu, S.; Ogura, K. *J. Am. Chem. Soc.* **1994**, *116*, 1151.

(5) (a) Yoshizawa, M.; Kusukawa, T.; Fujita, M.; Sakamoto, S.; Yamaguchi, K. *J. Am. Chem. Soc.* **2001**, *123*, 10454. (b) Kawano, M.; Kobayashi, Y.; Ozeki, T.; Fujita, M. *J. Am. Chem. Soc.* **2006**, *128*, 6558. (c) Dong, V. M.; Fiedler, D.; Carl, B.; Bergman, R. G.; Raymond, K. N. *J. Am. Chem. Soc.* **2006**, *128*, 14464. (d) Kuil, M.; Soltner, T.; van Leeuwen, P. W. N. M.; Reek, J. N. H. *J. Am. Chem. Soc.* **2006**, *128*,

11344. (e) Flapper, J.; Reek, J. N. H. *Angew. Chem., Int. Ed.* **2007**, *46*, 8590. (f) Lee, S. J.; Cho, S.-H.; Mulfort, K. L.; Tiede, D. M.; Hupp, J. T.; Nguyen, S. T. *J. Am. Chem. Soc.* **2008**, *130*, 16828. (g) Mal, P.; Breiner, B.; Rissanen, K.; Nitschke, J. R. *Science* **2009**, *324*, 1697. (h) Sarmentero, M. A.; Fernandez, P. H.; Zuidema, E.; Bo, C.; Vidal, F. A.; Ballester, P. *Angew. Chem., Int. Ed.* **2010**, *49*, 7489. (i) Cavarzan, A.; Scarso, A.; Sgarbossa, P.; Strukul, G.; Reek, J. N. H. *J. Am. Chem. Soc.* **2011**, *133*, 2848. (j) Horiuchi, S.; Murase, T.; Fujita, M. *J. Am. Chem. Soc.* **2011**, *133*, 12445.

(6) (a) Oxtoby, N. S.; Blake, A. J.; Champness, N. R.; Wilson, C. *Proc. Natl. Acad. Sci. U.S.A.* **2002**, *99*, 4905. (b) Campos-Fernandez, C. S.; Schottel, B. L.; Chifotides, H. T.; Bera, J. K.; Bacsa, J.; Koomen, J. M.; Russell, D. H.; Dunbar, K. R. *J. Am. Chem. Soc.* **2005**, *127*, 12909.

(7) Blake, A. J.; Champness, N. R.; Cooke, P. A.; Nicolson, J. E. B. *Chem. Commun.* **2000**, 665.

(8) (a) Lee, S. Y.; Park, S.; Kim, H. J.; Jung, J. H.; Lee, S. S. *Inorg. Chem.* **2008**, *47*, 1913. (b) Lee, J. Y.; Lee, S. Y.; Sim, W.; Park, K.-M.; Kim, J.; Lee, S. S. *J. Am. Chem. Soc.* **2008**, *130*, 6902.

(9) (a) Wang, M.-X.; Zhang, X.-H.; Zheng, Q.-Y. *Angew. Chem., Int. Ed.* **2004**, *43*, 838. (b) Yao, B.; Wang, D.-X.; Gong, H.-Y.; Huang, Z.-T.; Wang, M.-X. *J. Org. Chem.* **2009**, *74*, 5361. (c) Zhang, E.-X.; Wang, D.-X.; Huang, Z.-T.; Wang, M.-X. *J. Org. Chem.* **2009**, *74*, 8595.

(10) Wang, L.-X.; Wang, D.-X.; Huang, Z.-T.; Wang, M.-X. *J. Org. Chem.* **2010**, *75*, 741.

(11) (a) Wang, Q.-Q.; Wang, D.-X.; Ma, H.-W.; Wang, M.-X. *Org. Lett.* **2006**, *8*, 5967. (b) Yang, H.-B.; Wang, D.-X.; Wang, Q.-Q.; Wang, M.-X. *J. Org. Chem.* **2007**, *72*, 3757. (c) Wang, Q.-Q.; Wang, D.-X.; Zheng, Q.-Y.; Wang, M.-X. *Org. Lett.* **2007**, *9*, 2847.

(12) König, B.; Fonseca, M. H. *Eur. J. Inorg. Chem.* **2000**, 2303.

(13) Gong, H.-Y.; Zheng, Q.-Y.; Zhang, X.-H.; Wang, D.-X.; Wang, M.-X. *Org. Lett.* **2006**, *8*, 4895.

(14) Spek, A. L. *J. Appl. Crystallogr.* **2003**, *36*, 7.

(15) (a) Barbour, L. J. *J. Supramol. Chem.* **2001**, *1*, 189. (b) Atwood, J. L.; Barbour, L. J. *Cryst. Growth Des.* **2003**, *3*, 3.

(16) Wang, M.-X. *Chem. Commun.* **2008**, 4541.

(17) For some recent examples, see: (a) Cheng, J. K.; Yao, Y. G.; Zhang, J.; Li, Z. J.; Cai, Z. W.; Zhang, X. Y.; Chen, Z. N.; Chen, Y. B.; Kang, Y.; Qin, Y. Y.; Wen, Y. H. *J. Am. Chem. Soc.* **2004**, *126*, 7796. (b) Li, G. H.; Shi, Z.; Liu, X. M.; Dai, Z. M.; Feng, S. H. *Inorg. Chem.* **2004**, *43*, 6884. (c) Thébault, F.; Barnett, S. A.; Blake, A. J.; Wilson, C.; Champness, N. R.; Schröder, M. *Inorg. Chem.* **2006**, *45*, 6179. (d) Lee, S. Y.; Park, S.; Lee, S. S. *Inorg. Chem.* **2009**, *48*, 11335. (e) Manbeck, G. F.; Brennessel, W. W.; Evans, C. M.; Eisenberg, R. *Inorg. Chem.* **2010**, *49*, 2834.

(18) (a) Kiang, Y.-H.; Lee, S.; Xu, Z.; Choe, W.; Gardner, G. B. *Adv. Mater.* **2000**, *12*, 767. (b) Bonino, F.; Chavan, S.; Vitillo, J. G.; Groppo, E.; Agostini, G.; Lamberti, C.; Dietzel, P. D. C.; Prestipino, C.; Bordiga, S. *Chem. Mater.* **2008**, *20*, 4957. (c) Chavan, S.; Vitillo, J. G.; Groppo, E.; Bonino, F.; Lamberti, C.; Dietzel, P. D. C.; Bordiga, S. *J. Phys. Chem. C* **2009**, *113*, 3292. (d) Dietzel, P. D. C.; Besikiotis, V.; Blom, R. *J. Mater. Chem.* **2009**, *19*, 7362.

(19) (a) Zhao, B.; Gao, H.-L.; Chen, X.-Y.; Cheng, P.; Shi, W.; Liao, D.-Z.; Yan, S.-P.; Jiang, Z.-H. *Chem.—Eur. J.* **2005**, *12*, 149. (b) Baca, S. G.; Adams, H.; Sykes, D.; Faulkner, S.; Ward, M. D. *Dalton Trans.* **2007**, 2419. (c) Guo, Y.; Dou, W.; Zhou, X.; Liu, W.; Qin, W.; Zang, Z.; Zhang, H.; Wang, D. *Inorg. Chem.* **2009**, *48*, 3581. (d) Zhang, J.-Y.; Cheng, A.-L.; Sun, Q.; Yue, Q.; Gao, E.-Q. *Cryst. Growth Des.* **2010**, *10*, 2908.

(20) (a) Choi, H. J.; Suh, M. P. *J. Am. Chem. Soc.* **1998**, *120*, 10622. (b) Daiguebonne, C.; Guillou, O.; Kahn, M. L.; Kahn, O.; Oushoorn, R. L.; Boubekeur, K. *Inorg. Chem.* **2001**, *40*, 176. (c) Omata, J.; Ishida, T.; Hashizume, D.; Iwasaki, F.; Nogami, T. *Inorg. Chem.* **2001**, *40*, 3954. (d) Galan-Mascaros, J. R.; Dunbar, K. R. *Angew. Chem., Int. Ed.* **2003**, *42*, 2289. (e) Furukawa, S.; Ohba, M.; Kitagawa, S. *Chem. Commun.* **2005**, 865. (f) Rodriguez-Dieguez, A.; Cano, J.; Kivekaes, R.; Debdoubi, A.; Colacio, E. *Inorg. Chem.* **2007**, *46*, 2503. (g) Zhao, X.-Q.; Zhao, B.; Wei, S.; Cheng, P. *Inorg. Chem.* **2009**, *48*, 11048.

(21) (a) Syôzi, I. *Prog. Theor. Phys.* **1951**, *6*, 306. (b) Ramirez, A. P. *Annu. Rev. Mater. Sci.* **1994**, *24*, 453. (c) Grohol, D.; Papoutsakis, D.; Nocera, D. G. *Angew. Chem., Int. Ed.* **2001**, *40*, 1519. (d) Greedan, J. E. *J. Mater. Chem.* **2001**, *11*, 37. (e) Atwood, J. L. *Nat. Mater.* **2002**, *1*, 91. (f) Paul, G.; Choudhury, A.; Rao, C. N. R. *Chem. Commun.* **2002**, 1904. (g) Mekata, M. *Phys. Today* **2003**, *56*, 12. (h) Grohol, D.; Matan, K.; Cho, J.; Lee, S.; Lynn, J. W.; Nocera, D. G.; Lee, Y. S. *Nat. Mater.* **2005**, *4*, 323. (i) Lee, S.-H.; Kikuchi, H.; Qiu, Y.; Lake, B.; Huang, Q.; Habicht, K.; Kiefer, K. *Nat. Mater.* **2007**, *6*, 853.

(22) (a) Moulton, B.; Lu, J.; Hajndl, R.; Hariharan, S.; Zaworotko, M. J. *Angew. Chem., Int. Ed.* **2002**, *41*, 2821. (b) Perry, J. J.; McManus, G. J.; Zaworotko, M. J. *Chem. Commun.* **2004**, 2534. (c) Liu, Y. L.; Kravtsov, V. C.; Beauchamp, A.; Eubank, J. F.; Eddaoudi, M. *J. Am. Chem. Soc.* **2005**, *127*, 7266. (d) Wang, X.-Y.; Wang, L.; Wang, Z.-M.; Gao, S. *J. Am. Chem. Soc.* **2006**, *128*, 674. (e) Behera, J. N.; Rao, C. N. R. *J. Am. Chem. Soc.* **2006**, *128*, 9334. (f) Nytko, E. A.; Helton, J. S.; Müller, P.; Nocera, D. G. *J. Am. Chem. Soc.* **2008**, *130*, 2922. (g) Li, Z.-X.; Zhao, J.-P.; Sañudo, E. C.; Ma, H.; Pan, Z.-D.; Zeng, Y.-F.; Bu, X.-H. *Inorg. Chem.* **2009**, *48*, 11601. (h) Zhao, H.-R.; Li, D.-P.; Ren, X.-M.; Song, Y.; Jin, W.-Q. *J. Am. Chem. Soc.* **2010**, *132*, 18.

(23) Evans, O. R.; Lin, W. *Acc. Chem. Res.* **2002**, *35*, 511.

(24) (a) Fu, W.-F.; Gan, X.; Che, C.-M.; Cao, Q.-Y.; Zhou, Z.-Y.; Zhu, N.-Y. *Chem.—Eur. J.* **2004**, *10*, 2228. (b) Catalano, V. J.; Moore, A. L.; Shearer, J.; Kim, J. *Inorg. Chem.* **2009**, *48*, 11362.